Materials and Design 174 (2019) 107781

Contents lists available at ScienceDirect

Materials and Design

journal homepage: www.elsevier.com/locate/matdes

# Formation and homogenisation of Sn—Cu interconnects by self-propagated exothermic reactive bonding

Wenbo Zhu [a,b,c], Xiaoting Wang [a,c], Changqing Liu [c,*], Zhaoxia Zhou [d], Fengshun Wu [b]

[a] Material Science and Engineering, Harbin Institute of Technology, Shenzhen, China
[b] Material Science and Engineering, Huazhong University of Science and Technology, China
[c] Wolfson School of Mechanical, Electrical and Manufacturing Engineering, Loughborough University, United Kingdom
[d] Loughborough Materials Characterisation Centre, Department of Materials, Loughborough University, United Kingdom

## HIGHLIGHTS

- Sn—Cu bonds were developed by self-propagated exothermic reaction of AlNi NanoFoil.
- Nano-metastable phases were formed due to a non-equilibrium transient regime.
- The formation process is via convection diffusion and directional solidification.
- Nano-metastable phases were homogenised under an accelerated ageing.

## GRAPHICAL ABSTRACT

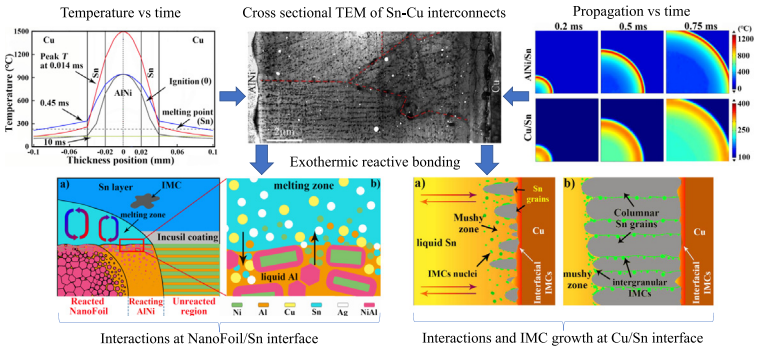


## ARTICLE INFO

*Article history:*
Received 12 January 2019
Received in revised form 30 March 2019
Accepted 5 April 2019
Available online 6 April 2019

*Keywords:*
Sn—Cu interconnects
Al-Ni NanoFoil
Exothermic reactive bonding
Non-equilibrium metastable phases
Interfacial reactions
Homogenisation

## ABSTRACT

We produced Sn—Cu interconnects by self-propagated exothermic reactions using Al—Ni NanoFoil at ambient conditions, through the instantaneous localised heat across the interfaces between Sn electroplated Cu substrates. This technique presents a great potential for electronics integration with minimal thermal effects to the components. However, the metastable phases resulted from the non-equilibrium interfacial reactions and solidification were inevitable under a highly transient regime due to a drastic heating/cooling (over $10^7$ K/s). In this study, Finite Element Analysis was performed to predict the temperature profiles across bonding interfaces, which were subsequently correlated with the formation and homogenisation of the bonded structures during the bonding and post-bonding ageing process. It has been revealed that, for nano-sized metastable phases, their formation, morphologies and distribution were primarily attributed to the convective mass transportation, liquid-solid inter-diffusion, and directional non-equilibrium solidification of Sn in molten zone of the bonding interfaces. The non-equilibrium phases initially formed in the Sn—Cu interconnects can be homogenised towards the equilibrium status by accelerated ageing. This was achieved through the coalescing and subsequent growth of the original nano-sized metastable phases, as a result of the solid-diffusion of Cu and Ag atoms at intergranular boundary regions of Sn grains, Al—Ni NanoFoil/Sn. and Cu/Sn interfaces.



* Corresponding author at: Wolfson School of Mechanical, Electrical and Manufacturing Engineering, Loughborough University, Loughborough, Leicestershire LE11 3TU, United Kingdom.
*E-mail address:* c.liu@lboro.ac.uk (C. Liu).

https://doi.org/10.1016/j.matdes.2019.107781

## 1. Introduction

Self-propagating exothermic reaction for synthesizing composite materials and intermetallic compounds has shown its effectiveness in providing a localised heating source for bonding various metals [1–6]. The reaction is based on an Indium NanoFoil® [7] prepared by vapour-deposition of hundreds of alternating layers at the nanoscale (e.g. Al—Ni, Al—Ti, and Al—Si). Once initiated with a small burst of energy in the form of either heat, electrical spark, laser or other means, the reaction starts due to a large enthalpy of mixing (e.g. 1050–1250 J/g for Al—Ni) and proceeds self-sustainingly at fast propagation velocities (7–10 m/s) [7–9]. The released energy is capable of melting adjacent metals followed by subsequent solidification creating a solid joint, thus known as reactive bonding.

Solder interconnects through reactive bonding, particularly with Al—Ni NanoFoils, offers numerous advantages [10–13]. The localised heat, extremely rapid heating/cooling under a steep temperature gradient towards adjacent regions can cause a small heat-affected zone (HAZ) [9,12]. This can reduce the ambient processing temperature, and achieve fluxless joining due to the breakdown of oxidation layers on the metal surface for bonding by significant transient thermal stress [6]. A buffer layer (normally metals) deposited on the substrate can create a transient zone to facilitate interfacial interaction to form a strong bond. This unique approach can enable the robust bonding of high-temperature Pb free solderable metals for heterogeneous integration of multi-functional devices.

J. Wang et al. bonded Au-coated stainless-steel specimens under ambient condition using free-standing Al—Ni multilayer foils and $Au_{80}Sn_{20}$ solder layers. The joints formed has enabled a 30% increase of the shear strength compared to conventional reflowed solder joints [11]. Bonding of bulk metallic glasses with an extremely high strength over 480 MPa, was also achieved by A. J. Swiston et al. using Al—Ni multilayer foils of 87–274 μm thick with 40–69 nm thick bilayer [3], where the structure of the glasses was not affected. T. Fiedler et al. successfully joined $Mg_{60}Cu_{40}Y_{10}$ with $Pd_{40}Ni_{40}P_{20}$ amorphous alloys using the reactive bonding technique [13] without forming a crystalline structure, and it has also been demonstrated to make strong bonds between Ti, ceramics, super-alloys and MEMS devices through reactive bonding with Al—Ni NanoFoils [1,4,14,15].

The exothermic thermodynamics of Al—Ni systems has been investigated experimentally and numerically. The diffusion-induced peritectic reaction has been counted for the reactive bonding process, primarily dominated by the heat conduction and the solid-liquid reactions between liquid Al and Ni nanolayers. However, the instantaneous and intensive nature of localised exothermic reactions can inevitably govern the interfacial reactions; hence the mechanical integrity of obtained interconnects. The heating rate of over $10^6$ K/s, followed by rapid cooling of up to 400 K/s [3], causes a drastic temperature gradient > $10^4$ K/mm across the bonding interface [11]. Under such conditions, the reactive bonding process is immensely non-equilibrium in the adjacent meals or alloys. For instance, the original nanolayers in multi-layered Al—Ni NanoFoils can be entirely replaced with coarsened and equiaxed NiAl grains after reaction based on an in-situ TEM observation [16]. In the $Au_{80}Sn_{20}$ based stainless-steel bonds, a fine lamellar microstructure (~50 nm spacing) and columnar inter-mixing regions at the Al—Ni NanoFoil/Au-Sn alloy interface were observed [11], with significant segregation of their composition in comparison with equilibrium Au—Sn alloys.

However, very little research has been performed to elaborate the interfacial interactions due to the exothermic reactive bonding, in particular, in the uses of such technique for electronics interconnects, where it is important to understand the fundamental details of such non-equilibrium process. In this study, bonding trails for Sn—Cu interconnect were implemented using the exothermic Al—Ni NanoFoil. Both computational and experimental approaches were carried out to examine the non-equilibrium exothermic reactive bonding process between Sn electroplated Cu substrates. Finite element analysis provides complementary, simulative insights into the localised temperature profiles and temperature gradients during the exothermic reactive bonding. The interfacial analysis using SEM/TEM and EDX techniques were also conducted to reveal the formation mechanism of non-equilibrium metastable phases and the microstructural homogenisation in the subsequent ageing process of the Sn—Cu interconnects.

## 2. Experimental details

As shown in Fig. 1(a), a 40-μm thick Al—Ni multi-layered NanoFoil® (Indium Corporation) with a 1:1 atomic ratio of Al to Ni consisting of alternating nanolayers of Al (60 nm thick) and Ni (40 nm thick) was used as the exothermic material. In the NanoFoil, 5 at. % Vanadium was added to refine the reaction products and improve the mechanical performance, with a 1 μm thick Incusil layer (59 wt% Ag-27.25 wt% Cu-12.5 wt% In-1.25 wt% Ti, an alloy used for high-temperature brazing) precoated on both side of the NanoFoil to protect the Ni or Al nanolayers from oxidation and providing a better wetting and reaction interface for common solder alloys [7]. As shown in Fig. 1(b), the NanoFoil was placed between two pieces 5 × 5 $mm^2$ Cu plates (Copper, 99.95%), 1 mm-thick as the bonding substrate, forming a sandwich bonding structure. The Cu plates were coated with 20 μm-thick electroplated Sn layer composed of fine equiaxed Sn grains, η-$Cu_6Sn_5$ IMC particles, and a continuous 0.5 μm-thick interfacial η-$Cu_6Sn_5$ layer (Fig. 1(c)). NanoFoil inserted was slightly larger (5 × 7 $mm^2$) than Cu plates thus accessible for ignition through electrical discharge.

The reactive bonding was implemented under the ambient condition using 1 MPa pressure and 373 K preheating, the optimal parameters as previously determined [17]. The exothermic reaction was initiated by an electrical spark produced through a DC power supply at 5 V and 1A.

Finite element analysis (FEA) was performed based on a simplified description of the exothermic reactions, using the finite element equations in the Heat-Transfer in Fluids module of COMSOL Multiphysics, the typical heat conduction equation, $\dot{q} = \rho Cp(\partial T/\partial t + v_x \partial T/\partial x + v_y \partial T/\partial y + v_z \partial T/\partial z) + \rho \Delta H_f - \lambda Cp \nabla^2 T$ [18,19], and the convective heat transfer equation, $\rho C_p \partial T/\partial t + \rho C_p u \cdot \nabla T + \nabla \cdot q = Q + Q_\rho + Q_{vd}$, $q = -k \nabla T$, where $\dot{q}$ is the heat releasing rate, Cp is the heat capacity, $t$ is the time, $\rho$ means the density, $v_{x,\,y,\,z}$ is the reaction velocity, and $\Delta H_f$ represents the latent heat of melting. The simulation primarily focused on the prediction of the temperature profiles across the bonding interfaces, which is dominated by the heat released from the exothermic reaction ($\dot{q}$) and the (convective) heat transfer among materials [6,20], as a controlling factor of the interfacial reactions and phase evolution. To this end, the exothermic reaction was set as a function of time and axis based on the moving heat source method, of which the heat releasing rate was assumed to be uniform in the thickness direction and localised within the reacting area. The thermal conduction across the materials and a hypothesised conductive heat transfer inside the solder layer were also considered using the fluid properties of Sn-based solders from the previous research of Shang and T. Gancarz [21,22], while the trapped air, impurities, atomic inter-diffusion, phase evolution and physical motion of solids in fluids were neglected. The FE model had been validated by measuring temperature at specific locations inside the substrate, of which the measured data had an almost identical long-term temperature evolving trend and a small deviation in maximum temperature (<3%, e.g. 118 °C and 84 °C from prediction, and 119 °C and 83 °C by measurement, respectively) with the predicted results [19].

A FEI Nova 600 Nanolab dual-beam Focused Ion Beam/Scanning Electron Microscope (FIB/SEM) was employed to lift-out cross-sectional TEM samples across the interfaces of bonded structures. The thin samples of approximately 100 nm-thickness were mounted on molybdenum (Mo) supporting grids and examined using a FEI Tecnai F20

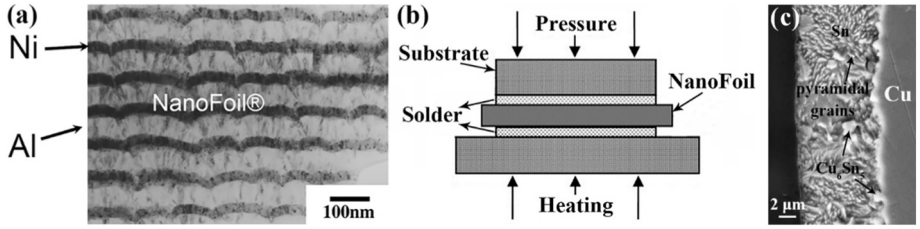


**Fig. 1.** (a) Cross-section morphology of Al—Ni NanoFoil, (b) Schematic sandwich bonding structure, (c) SEM cross-section of Sn-plated Cu plates as bonding substrate.

TEM equipped with Oxford Instruments X-max$^N$ 80 TLE SDD detector for compositional mapping by energy dispersive X-ray analysis (EDX). The TEM was operated in scanning mode at 200 kV with a scanning probe tuned to be ~2 nm. High angle annular dark field (HAADF) images were recorded together with the chemical maps. Then, the bonded structures were subjected to an accelerated ageing test at 175 °C for the various time in order to understand the thermal effects on the microstructural evolution. The TEM samples were aged for 5, 15 and 30 mins, while the as-bonded joints were aged for 2, 8, 24, 72 h for various analysis and mechanical testing. The shear tests were also conducted on these as-bonded and aged sandwich bond structures using a DAGE 4000+ tester at a shear speed of 5 μm/min.

## 3. Results

### 3.1. FEA of bonding temperature profiles

The time-dependent FEA of the temperature profiles across the reactive bonding interfaces of the Cu/Sn/NanoFoil/Sn/Cu sandwich structure (Fig. 2(a) and (b)) indicates the local temperature increases abruptly at the reaction front with the propagation progresses. The exothermic reaction was completed at 0.014 ms, where the maximum temperature 1765 K can be attained in NanoFoil at an average heating rate of $10^{6-7}$ K/s. A drastic temperature decrease, down to 1434 K at the NanoFoil/Sn interface and 539 K at the Sn/Cu interface, causes a steep temperature gradient, $3.06 \times 10^7$ K/m, extended into the Sn layer. Meanwhile, with a less steep gradient in the Cu within 60 μm, the temperature levels off to ambient temperature. After the temperature at the Sn/substrate interface reaches its peak point, 610 K, at 0.45 ms, the Sn layer remains molten until the temperature drops sharply to 505 K within 0.226 ms, with a cooling rate about $10^{5-6}$ K/s. Because of the rapid heating and cooling, the interfacial reactions and crystallization of metals can be of highly non-equilibrium. The planar temperature distributions at both NanoFoil/Sn and Sn/Cu interfaces (Fig. 2(b)) shows the peak temperature proceeds with propagation front (Fig. 2(b)). However, the heat released from the exothermic reaction (~$3.9 \times 10^8$ W/cm$^3$) is far outweighed the heat transfer capability of the Sn (66.8 W/m·K), causing a severe heat accumulation in the Sn layer, at a gradient of up to $10^7$ K/m, compared with the $10^5$ K/m in the Cu substrate.

### 3.2. Microstructural characteristics of interconnects

TEM cross-sectional view of the bonded structure revealed the fine NiAl—grains with an in-plane size of 30–100 nm formed in the NanoFoil after reaction (Fig. 3(a)), which was in contact and bonded with the compact Sn layer (Fig. 3(b)). In the Sn layer, submicron long-thin columnar grains with nano-sized intergranular IMC precipitates at the grain boundary were observed. These grains formed as groups at different orientations, the boundary-like domains. The EDX results in Table 1 confirmed the columnar grains are composed of Sn with trace Ni, Cu and Ag, whilst both the intergranular IMCs and boundary-like domains consist of non-stoichiometric phased of $CuSn_{2-4}$ or $AgSn_{1-3}$, which cannot be found in the phase diagrams and are hence deemed to be metastable. Among these Sn grains and IMCs, voids with a dimension of up to tens of nanometres were observed, likely due to the rapid volume shrinkage at the cooling transient stage.

Further details of the NanoFoil/Sn and Sn/Cu interfaces are revealed through HAADF analysis in Fig. 4. Clearly, at the NanoFoil/Sn interface (Fig. 4(a), (b) and (c)), a 10–20 nm-thick interfacial Cu-rich IMC layer was indicative of the annihilation of the Ag59-Cu27.25-In12.5-Ti1.25 Incusil metallization due to the exothermic reaction. The formation of significant Ag-enriched IMCs in the Sn layer confirms the dissolution and migration of Ag from the Incusil coating. However, the multilayered structures of Ni—Al foils remains in the mixture with the equiaxed NiAl grains resulted from the exothermic reaction, whilst an inter-diffusion region (~100 nm) can be seen between the NanoFoil and Cu-rich IMC layer. The inter-diffusion region was found to contain Ag, Sn and Cu, surrounded by Al-enriched segregations, suggesting a considerable atomic scale diffusion of Sn into NanoFoil.

At Sn/Cu interface (Fig. 4(d), (e) and (f)), discrete η-$Cu_6Sn_5$ IMC grains in the Sn layer, with metastable $CuSn_{1-2}$ IMCs distinctive from the continuous IMC layer are evident. In addition, the grain refinements

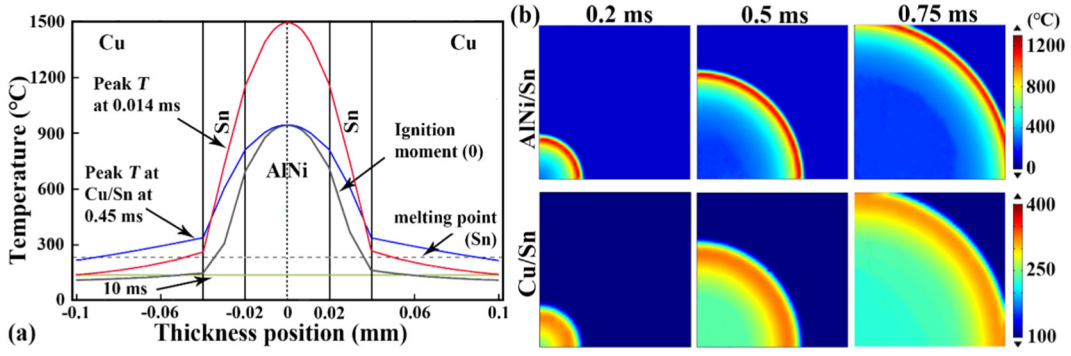


**Fig. 2.** (a) Perpendicular temperature profiles across bonding interfaces after different time, and (b) Planar temperature distribution at the NanoFoil/Sn and Sn/Cu interfaces at propagation front 0.2, 0.5, 0.7 ms after ignited.

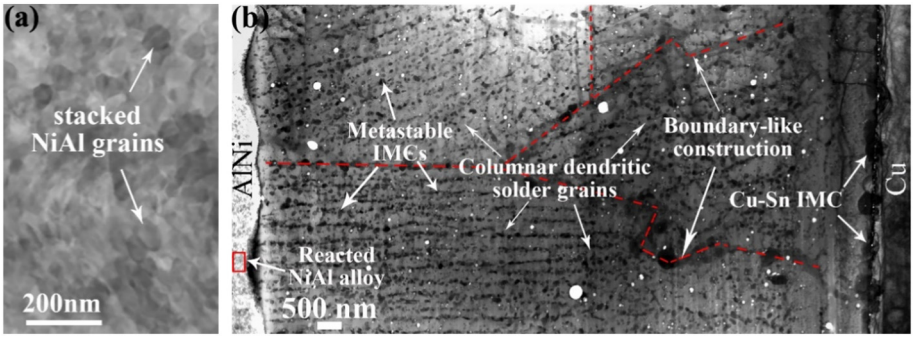


**Fig. 3.** Cross-sectional TEM: (a) NanoFoil after the reaction, and (b) Electrodeposited Sn layer between the NanoFoil and Cu substrate.

**Table 1**
Cross-sectional TEM-EDX elemental analysis of the bonded structures (at. %).

| Testing locations | Cu | Ag | Sn | Ni | Al |
|---|---|---|---|---|---|
| Columnar Sn grains | 0.4–3.2 | 0–2.0 | 94.7–99.2 | 0.2–3.8 | 0–2.3 |
| Intergranular Cu—Sn IMCs | 18.4–41.1 | 0–0.9 | 50.1–73.0 | 2.6–7.3 | 0–2.1 |
| Intergranular Ag—Sn IMCs | 3.1–12.7 | 29.2–54.6 | 35.1–63.2 | 1–5.9 | 0–2.2 |

of Cu near the interface are also observed as a result of heat effect due to the exothermic reaction.

### *3.3. Effect of thermal ageing on microstructural characteristics of the Cu—Sn interconnects*

SEM morphological evolution of the bonds due to the ageing (Fig. 5 (a)) clearly shows the growth of Cu—Sn IMCs at the Cu/Sn interface with the ageing time, but hardly observed at NanoFoil/Sn interface. In the Sn layer, after long time 72 h ageing, only small numbers of IMCs particles of hundreds of nanometers remain, of which the dark phases were identified to be η-$Cu_6Sn_5$ and the bright particles were the $Ag_3Sn$. At the Cu/Sn interface, the thickness of the interfacial IMCs (fully η-$Cu_6Sn_5$) layer increased exponentially with ageing time, and a ε-$Cu_3Sn$ layer was gradually appeared and grow between η-$Cu_6Sn_5$ and Cu, as observed in the conventional interconnects formed by, for instance, reflow process.

However, in-situ TEM analysis of the interconnects with ageing in Fig. 5(b)) has revealed that, even within 15 min of ageing, the nano-sized intergranular metastable IMC precipitates had been dissolved into the Sn matrix, as evidenced by the significantly decreased number of Ag—Sn and Cu—Sn IMCs. This is particularly true near the Cu/Sn interface accompanying the growth of interfacial IMCs. However, in the Sn layer, it appeared these metastable IMC precipitates had migrated to the boundary-like regions and merged into large sizes of IMCs with an increased Cu/Ag concentration (near-equilibrium). When the ageing was long enough, the concentration of Sn (Ag, Cu) at the inter-diffusion region decreased evidently, and equilibrium IMC particles up to 300 nm can be formed. However, no noticeable changes of IMCs layer have been found at NanoFoil/Sn interface, apart from a seeming growth of a void locally. It can also be expected that the dissolution of Incusil coatings and metastable IMCs at NanoFoil/Sn interface can be homogenised due to ageing.

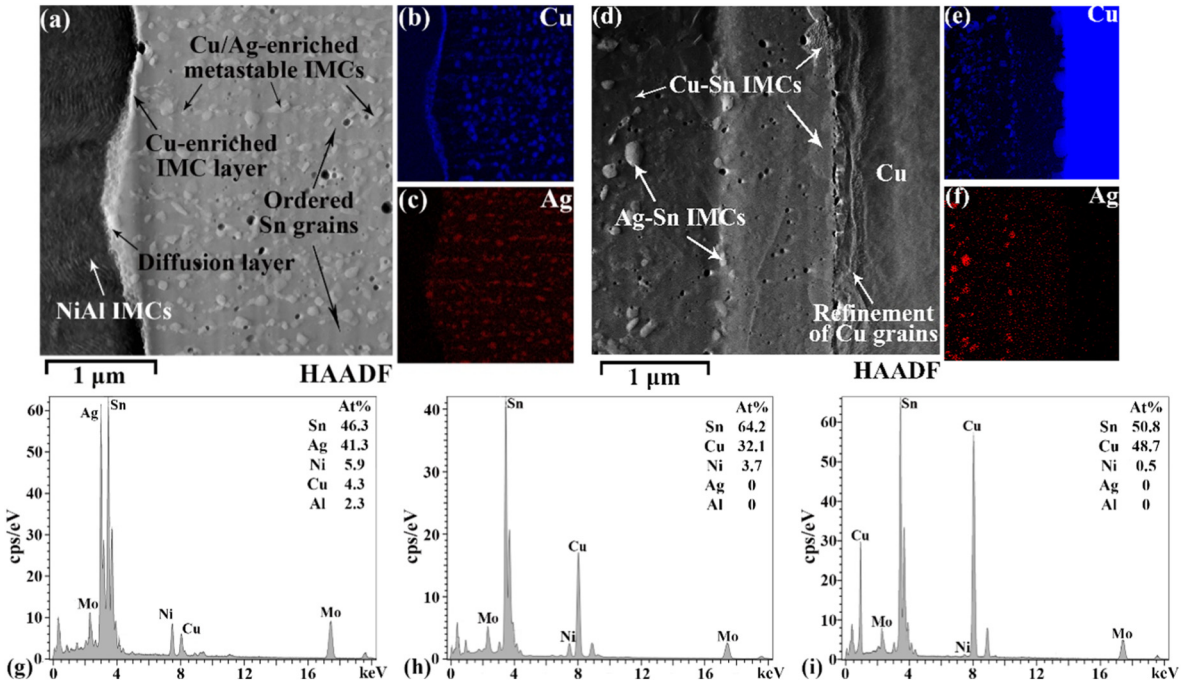


**Fig. 4.** TEM HAADF and EDX mapping of phases at the NanoFoil/Sn (a–c) and Sn/Cu (d–f) interfaces. The formation and orderly distribution of Cu—Sn and Ag—Sn phases in the Sn layer were identified. The elemental analysis of Ag-enriched IMCs (g), Cu-enriched IMCs (h) in the Sn layer and the interfacial IMCs on Cu substrate (i) indicates these IMCs have a different composition from those presented in the equilibrium phase diagram.

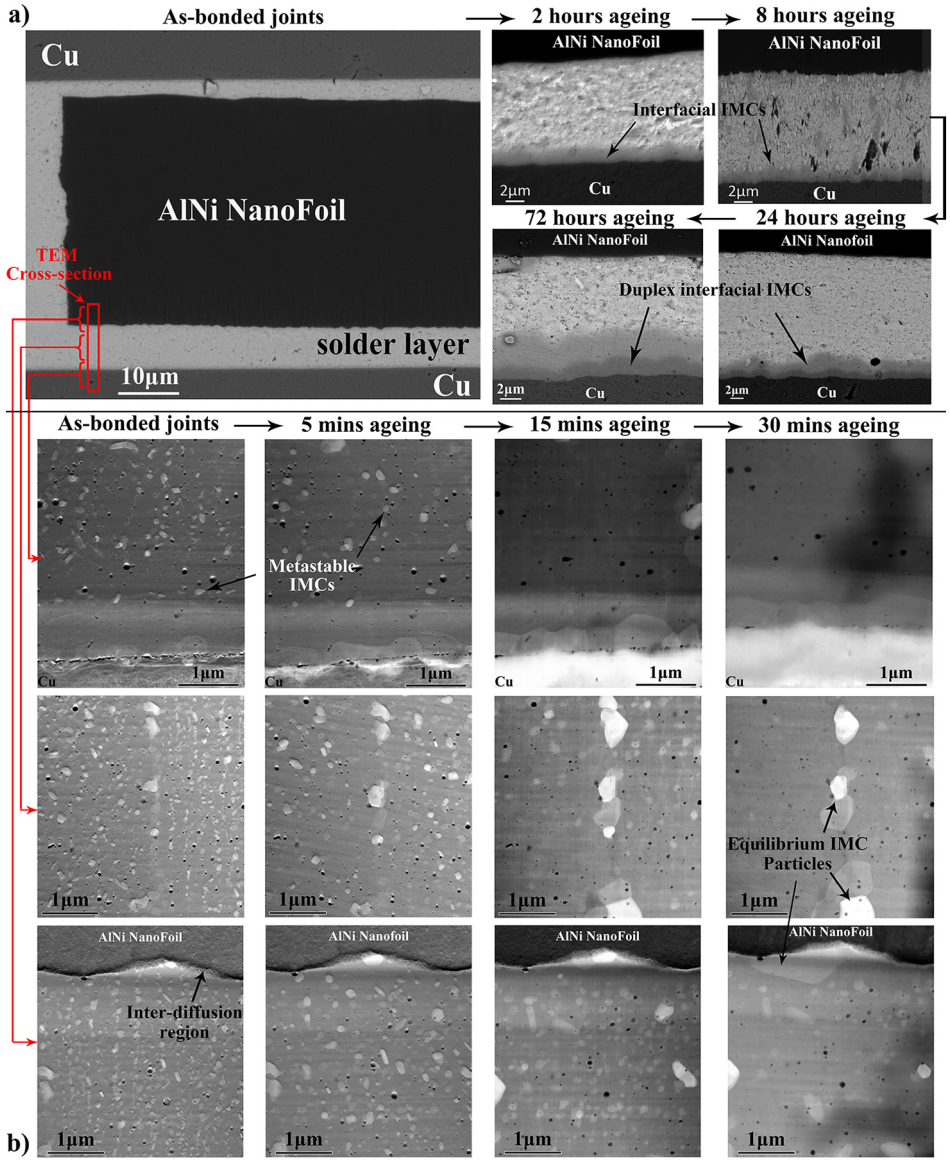


**Fig. 5.** (a) Morphological SEM of Cu-Sn-NanoFoil interconnect before and after 175 °C ageing for 2, 8, 24 and 72 h, and (b) in-situ cross-sectional TEM analysis on the Sn layer, NanoFoil/Sn and Cu/Sn interfaces after 175 °C ageing for 5, 15 and 30 min.

Further analysis of the constituents in the IMCs by EDX in TEM shows the changes in atomic ratios of Cu, Ag and Sn in the IMCs at different locations (Fig. 6(a) and (b)). Overall, across the entire Sn layer from AlNi NanoFoil to Cu substrate, the Cu content in Cu—Sn IMC or the Ag in Ag—Sn IMCs increases with ageing time, because non-equilibrium IMCs formed due to insufficient inter-diffusion during the limited time of exothermic reaction were homogenised from metastable status to become more stabilised. However, the solute ratio of Cu which also co-existed in the solidified columnar Sn grains slightly increased in the central Sn layer and near the NanoFoil, but drastically decreased near Cu substrate during the ageing process (Fig. 6(c)). This is expected as the result of the transformation from non-equilibrium to stable phases owing to the continuous supply of Cu from the substrate. Nevertheless, it is hard to see any major changes for the solute element Ag in the Sn grains due to ageing, primarily due to the limited amounts of Ag available in the 1 μm thick Incusil layer.

The compositions of the interfacial IMCs at both NanoFoil/Sn and Cu/Sn interfaces were also homogenised with the ageing time (Fig. 6(d)). With the significant increase of Ni and reduction of Sn and Cu, the initial continuous $(CuNi)_6Sn_5$ layer with the embedded $Ag_3Sn$ particles at the NanoFoil/Sn interface evolves with ageing time till they reach the equilibrium status. However, at the Cu/Sn interface, as expected, the Cu content in the IMCs slightly increases, but the element Sn decreases with the ageing time. This is likely attributed to the formation of $Cu_3Sn$ through further diffusion and supply of Cu from the substrate, and the conversion of initial $Cu_6Sn_5$ IMCs into $Cu_3Sn$ as the IMCs layer continues to grow thicker.

### 3.4. Effect of thermal ageing on the shear strength of the interconnects

The experimental results from the shear tests of the bonded structures were collected and plotted in Fig. 7. Clearly, the shear strength reached the peak point after aged for 24 h, showing an approximately 20% increase from 21 MPa to 25 MPa, and this was followed by a drastic decrease thus arrived at the lowest point, 16 MPa. After 120 h ageing, the shear strength remained more or less unchanged. Such changes in the bonding strength should reflect the microstructural evolution, i.e. equilibration, morphological characteristics and growth of IMCs.

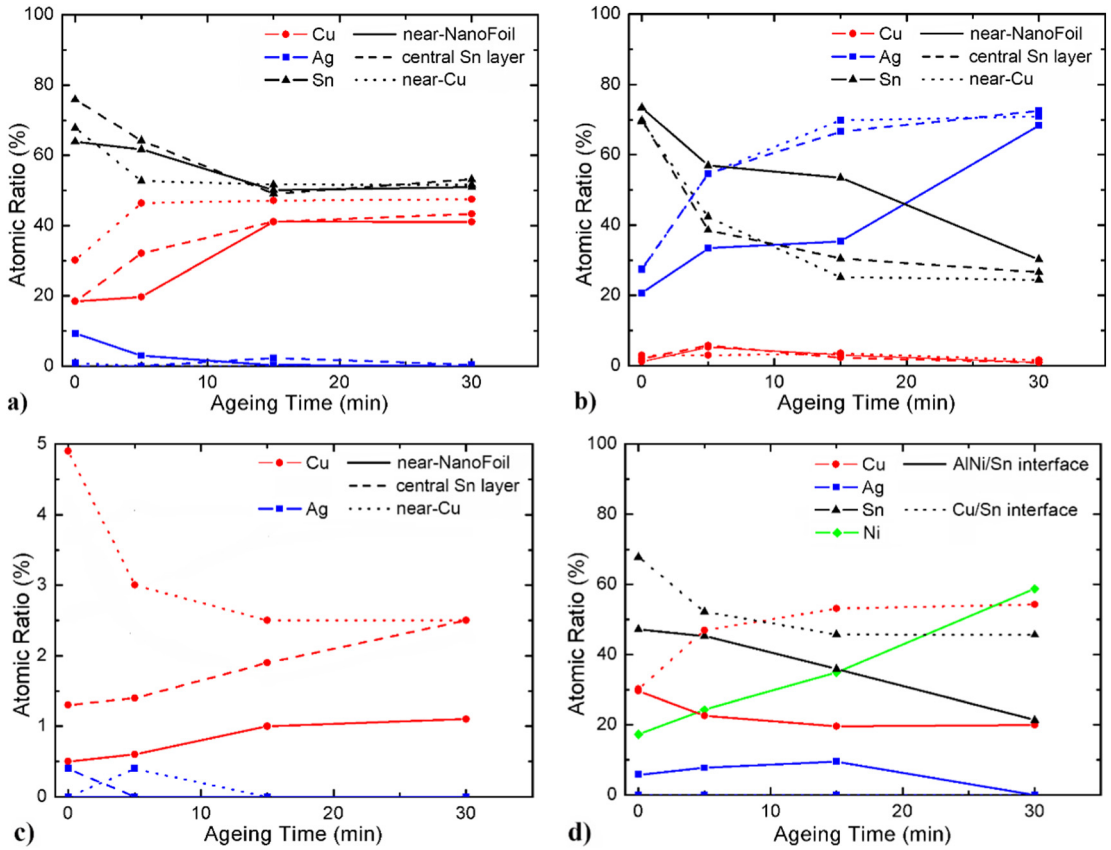


**Fig. 6.** EDX analysis in TEM on the constituents (Cu, Ag and Sn) in IMCs with ageing time: (a) Cu—Sn IMCs precipitates, (b) Ag—Sn IMCs precipitates, (c) Solute Cu and Ag in the Sn grains across the Sn interconnect layer, and (d) Interfacial IMCs formed at AlNi NanoFoil/Sn and Cu/Sn interfaces.

## 4. Discussion

Considering the diffusivity of Ni in liquid Al ($0.386–1.8 \times 10^{-8} m^2 s^{-1}$ in the range of 980–1773 K), Cu and Ag in liquid Sn ($0.413–1.075 \times 10^{-8} m^2 s^{-1}$ in the range of 560 K to 750 K, and $0.59–1.18 \times 10^{-8} m^2 s^{-1}$ in the range of 560 K to 1108 K, respectively) [23], the diffusions of Ni, Cu and Ag are expected to be within the range of tens of nanometres during self-propagating reaction. However, Table 1 clearly shows the IMCs were enriched by Ag and Ni across the entire Cu—Sn interconnected structures, primarily in the form of intergranular IMCs precipitates along the grain boundaries (Fig. 3). This implies the elements such as Ni, Ag, Cu must migrate through an entirely different mechanism across the 20 μm-thick Sn layer between NanoFoil and Cu substrates, which could have ~$10^3$ higher speed than the solid-liquid diffusion process. Among a variety of potential routes, the model of the convective motion of liquid [16] can be confirmed to enable such fast

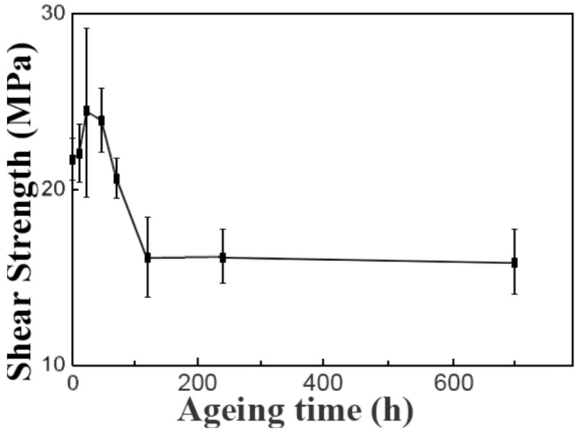


**Fig. 7.** Shear strength of bonded structures after aged at 175 °C for up to 720 h, from which a fluctuation in strength was detected after the different time of ageing.

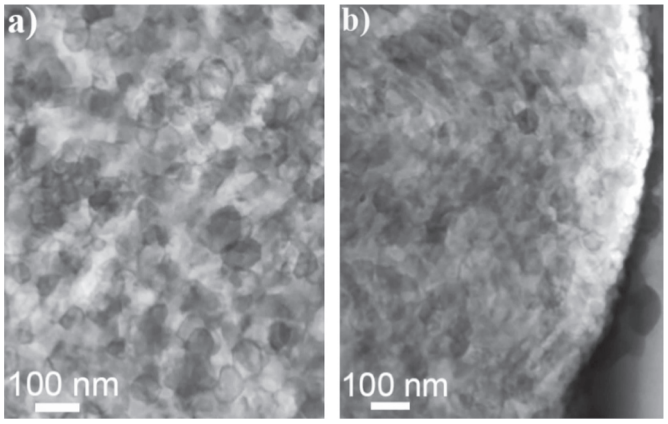


| At. % | Ni | Al | Others (Sn/Ag/Cu) |
|---|---|---|---|
| a) | 50.48 | 49.52 | 0 |
| b) | 45.7 | 25.7 | 28.6 |

**Fig. 8.** The two types of NiAl grains formed after exothermic reaction: (a) equiaxed IMCs in the central part due to complete reaction; and (b) orderly assembled lamellar NiAl nano grains near the NanoFoil/Sn zone due to incomplete reaction.

transportation of the elements across the Sn layer; this is supported by the numerical predictions of temperature profiles (Fig. 2(a)). The extreme high localised temperatures can melt the entire Sn layer instantaneously. The re-distribution and mass transfer of individual components can occur given the micro-scale thermal gradients and the applied pressure. These can force the convective motion of the molten Sn, facilitating a long-range atomic migration across the Sn layer, forming non-equilibrium metastable phases through simultaneous solidification as the exothermic reaction propagates further at the front of the bonding.

### 4.1. Transformation of NanoFoil through the exothermic reaction

Phase transformation of a single Al—Ni NanoFoil in the exothermic reaction, as reported in [16], is accomplished through the peritectic reaction between Ni and Al nanolayers by the active solid-state diffusion upon the ignition with heating (i.e. 493 K) or sparks. This reaction spontaneously produces localised energy to rapidly heat up the NanoFoil and accelerate the Al—Ni inter-diffusion process [9,16]. The heat generated is sufficient to melt the Al nanolayers initiating the convective motion of liquids in the solid-liquid mixture under the thermal transient stress developed between nanolayers. The transient stress and the volume reduction induced by the formation of NiAl IMCs can fragment Ni nanolayers into fine solid Ni nano-particles. As inter-diffusion regions between Ni and Al expand, a drastically increased temperature at the central area of the NanoFoil could exceed the melting point of Ni (1728 K), which allows the complete Ni—Al reaction in the liquid state, forming nano NiAl IMC grains by cooling. Due to the primarily homogeneous nucleation, the equiaxed IMCs nano-grains with random orientations were observed in the central part of the NanoFoil after solidification (Fig. 8(a)). However, since the temperature in the region near the NanoFoil/Sn interface, which is ~1434 K, may not exceed the melting point of Ni and NiAl IMCs, the incomplete Ni—Al reaction of nanolayers was expected. This can result in a mixture of liquid Al with a wide range of solid components including fragmented Ni and NiAl IMCs nano-particles, where further refinement and alignment of these mixed nano-grains due to the solidification under fast cooling and the steepest thermal gradient resulted in the lamellar textures (Figs. 4(a) and 8(b)). The EDX results in the table of Fig. 8 confirm that the NiAl atomic ratio of the reacted NanoFoil near the NanoFoil/Sn interface was significantly higher than that in the central part of the reacted NanoFoil, indicating the incomplete Ni—Al reactions in this zone. In addition, as can be expected, substantial other metallic elements such as Sn, Ag and Cu had penetrated into the NanoFoil through the convective motion of liquid phases as proposed above.

### 4.2. Interfacial interactions in exothermic reactive bonding and formation of Cu—Sn interconnects

Given the combined liquid phases such as Al in NanoFoil, the elements in the Incusil coatings (melting point is 988 K) and Sn with the fragmented Ni or NiAl solid nanoparticles makes a mushy status at the NanoFoil/Sn interface zone, the proposed solid-liquid diffusion through the convective mass transportation in the liquids is most likely to cause the atomic migration which can in turn govern the interfacial interactions (Fig. 9(a)). As stated above, the incomplete Ni—Al reactions near the NanoFoil/Sn interface cause a mixture of multiple phases, likely in two forms, i.e. NiAl IMC particles and NiAl-Ni core-shell particles in an orderly alignment (Figs. 4(a) and 8(b)). Taking the local mushy region at NanoFoil/Sn interface, one can propose the interactions of multiple components through convective motion schematically shown in Fig. 9(b). The convective flow in this zone can assist to release the transient thermal stress and change the density of different liquids; as such the elements from the NanoFoil, Incusil coating and Sn can lead to the formation of interfacial high-melting-point metastable IMCs, i.e. $(CuNi)_6Sn_5$ and $Ag_3Sn$ (Fig. 6(d)). The Cu atoms could be supplied from Incusil layer, and possibly transported directly from Cu substrate, through the 'nearest neighbour jump' mechanism [24–26].

However, given the transient nature of propagating bonding process, the rapid heating and cooling do not permit sufficient time for elemental redistribution or further growth of the phase precipitates (e.g. IMCs) once formed. The preferential transient state aggregations of these IMCs along the columnar Sn grain boundaries are likely to occur forming the non-equilibrium metastable IMC phases under the extremely high temperature gradient [27–30].

The solid-liquid convective inter-diffusion process also occurs through the interfacial reactions at the Sn/Cu interface. Firstly, the high temperature at this region can exceed the melting point of original $Cu_6Sn_5$ IMCs (Fig. 2), which is likely to dissolve the original IMCs and restart the reactions with the molten Sn. This can induce a solute Cu enrichment, which causes the formation of a large number of high Cu content IMC particles, particularly due to the limited time for Cu to be redistributed through the fast cooling and solidification, and formation of the IMCs particles accompanies with the nucleation and growth of Sn grains (Fig. 10(a)). Akin to the IMCs formed at the NanoFoil/Sn interface, these IMCs could not fully reach the equilibrium state, but a continuous quasi-equilibrium $\eta$-$Cu_6Sn_5$ IMCs layer could be formed and grow thicker at the Cu/Sn interface (Fig. 5(a)), given sufficient element source and relatively longer interaction time. The heat generated by exothermic reaction can also anneal the surface of the Cu substrate, i.e. causing the grain refinement, the lattice distortion of Cu grains and numerous vacancies, even dislocations [31–33].

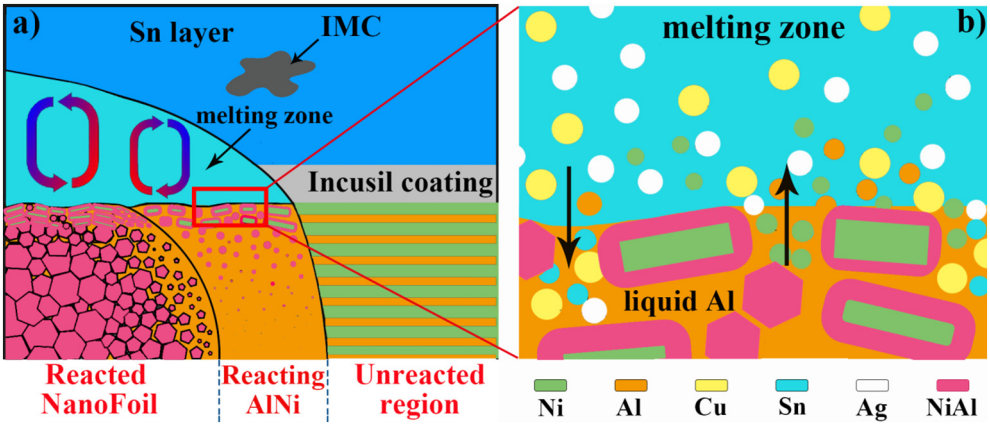


**Fig. 9.** Schematics of the inter-diffusion in the mushy zone between NanoFoil and molten Sn layer through the solid-liquid-convective diffusion of multiple components, (a) an overview of the front point of propagating exothermic reactions, (b) interactions of multiple components in the mushy zone.

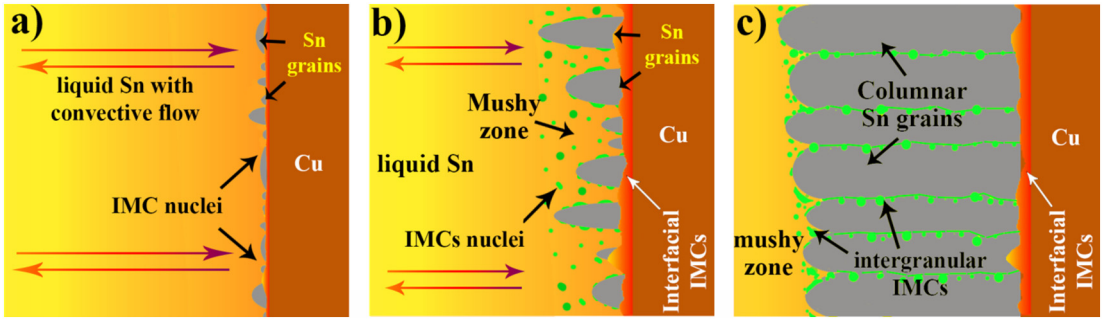


**Fig. 10.** Schematics of the inter-diffusion between Cu substrate and molten Sn layer through the solid-liquid-convective diffusion of multiple components, (a) initial nucleation stage of Sn grain and IMCs particles at the front point of propagating exothermic reactions, (b) directional growth of columnar Sn grains and interfacial IMCs layer, (c) aggregation of IMCs precipitates forming intergranular IMCs along the Sn grain boundaries.

The formation of columnar Sn grains with the nano-sized IMCs aggregated along the grain boundaries is expected under the non-equilibrium transient state in the mushy zone (Fig. 10(b)). This could be initiated from the Cu substrate, given the steep temperature gradient and rapid cooling, the Cu, Ag enriched IMCs (Fig. 6(a) and (b)) which had high melting temperature can thus be formed in the mushy zone.

These Sn grains solidify and grow rapidly but directionally forming long thin columnar structures, given the great heat dissipation along the perpendicular direction to the Cu/Sn interface [34]. The IMC precipitates are expected to aggregate at grain boundaries to minimize the interfacial energy in the mushy zone, hence forming the intergranular IMCs after solidified (Fig. 10(b) and (c)) [35]. Similar to the IMC phases formed at both NanoFoil/Sn and Cu/Sn interfaces, the elemental redistribution and subsequent growth of Sn grains and IMCs in the intergranular region cannot be fully complete due to the transient heating and cooling nature of reactive bonding. This explains why a number of components and IMCs in the as-bonded Sn—Cu interconnects primarily consist of metastable phases at the nanometre scale.

### *4.3. Microstructural homogenisation of Sn—Cu interconnects by ageing*

Accelerated ageing process allows the nano-scale non-equilibrium metastable phases to be fully homogenised towards the equilibrium status, and this has been observed by the merging and growth of the IMCs (Fig. 4(b)). This can be quantitatively evaluated by counting the number of IMCs and measuring their mean value of size with ageing time as statistically derived in Fig. 11(a). The evolution of the IMCs has been completed through the dissolution, equilibration and final growth almost occurring simultaneously, with the composition and energy states being varied at different locations. While the pronounced nano-scale IMCs precipitates exist prior to or after a short time (e.g. 5 mins) ageing, with the ageing time further extended, the merging and subsequent growth of these original IMCs are apparent (Fig. 11(a)). Driven by compositional gradients in each component IMCs or Sn grains, the solid-diffusion of Cu and Ag atoms from metastable IMCs and intergranular regions into Sn can take place [36], leading to the homogenisation of entire Sn—Cu interconnect at elevated temperature (Figs. 5 and 6). The relation of mean IMC size vs ageing time embedded in Fig. 11(a) indicates the IMCs increases from the initial 50 nm to ~200 nm as the result of ageing.

Similarly, at the NanoFoil/Sn and Cu/Sn interfaces, the IMCs evolve with ageing time as the homogenisation process. The "over-saturated" atoms from the inter-diffusion region and substrate, serving as elemental sources, enable the atomic replacement in metastable IMCs. As a consequence, the concurrent homogenisation and growth of interfacial IMCs were evident, which abides the kinetics which substantially differentiates from the one with originally equilibrium IMCs, for instance, in the case of Sn joints formed by conventional reflow process (Fig. 11(b)). In particular, it is interesting to observe a significant change of kinetics of the IMCs growth at Cu/Sn interfaces, which is likely due to the availability of the large amount of solute Cu to reach their equilibrium status. Given the thickness of IMC layers, the growth rates of interfacial IMCs with ageing time, especially in the short-term ageing, can be calculated, and the result indicates the value is much greater than what has been reported for reflow soldering [37]. The increased growth velocity is likely attributed to the presence of the non-equilibrium metastable IMCs formed during propagating exothermic reaction. According to the Arrhenius equation, the growth constant of phases was dominated by the activation energy that is responsible for the interfacial reactions to form IMCs. In the case of metastable IMCs, their Gibbs free energy was lower than the original Sn but much higher than the relevant equilibrium IMCs, such that less activation energy is required to complete

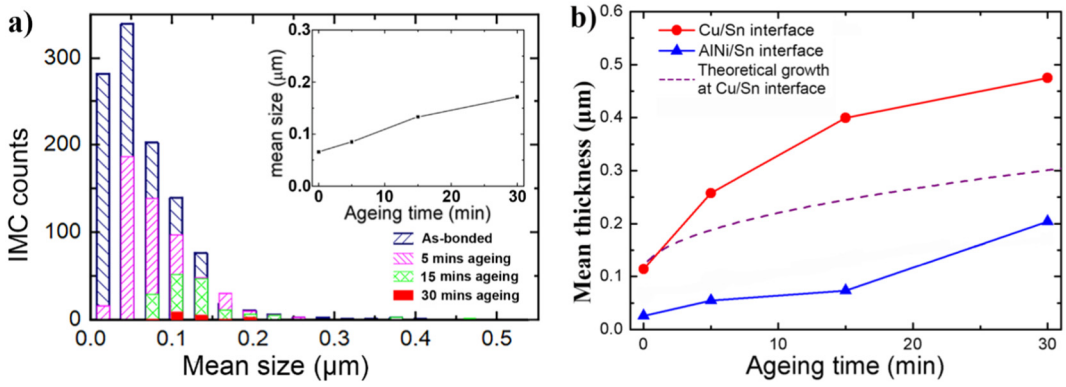


**Fig. 11.** (a) Average IMC counts by ImageJ with ageing time in the Sn—Cu joints, and (b) IMCs thickness vs ageing time at both NanoFoil/Sn and Cu/Sn interfaces with reference of IMC growth of conventional reflow Sn joint.

the growth [38]. The formation and growth velocity of IMCs can, therefore, be accelerated, leading to a relatively thicker IMC layer than conventional Cu—Sn interconnects given the same ageing conditions at the initial ageing period since the metastable IMCs are not fully equilibrated.

The fluctuation of the measured shear strengths of the aged Cu—Sn joints in Fig. 7 was resulted from the microstructural evolution and homogenisation. From the SEM images in Fig. 5(a), the initial voids formed mainly at the interfaces during the bonding process were reduced at the initial ageing stage, possibly due to the atomic migration and growth of phases occurred in the homogenisation process. This can be correlated with the initial shear strength increase in Fig. 7. However, further extended ageing time can cause significant CTE mismatch and induce the interfacial "Kirkendall voids" due to extensive diffusion process [39], thus leading to the deterioration of the mechanical strength of the Sn—Cu interconnects (Fig. 7).

## 5. Conclusions

To summarise, we have successfully developed an ambient bonding process to form the Sn—Cu interconnects through self-propagating exothermic reactions. For the optimal design of the bonding structures and processing parameters, the formation and subsequently homogenisation of Sn—Cu interconnects have been investigated to understand the interfacial interactions and phase transformations during the bonding and subsequently ageing processes. Both FEA simulations and SEM/TEM analysis confirmed that the metastable and very often non-stoichiometric IMCs was formed through a non-equilibrium process at an extremely short time (~0.014 ms). This was involved with the liquid-solid diffusion and convective mass transportation of multiple components in the mushy zone of NanoFoil/Sn and Cu/Sn interfaces at the propagating front point.

It has been found that the incomplete Ni—Al reaction near the NanoFoil/Sn interfaces resulted in a mushy zone of an orderly aligned residual fragmented Ni and NiAl IMC-Ni core-shell particles. This has caused non-equilibrium metastable IMCs and their insufficient growth and aggregations through a transient phase transformation due to the rapid heating and cooling. The solid-liquid convective inter-diffusion at the Sn/Cu interface also produced a solute Cu enrichment in the IMC particles precipitated alongside the grain boundaries of columnar Sn under the high perpendicular temperature gradient. However, a continuous quasi-equilibrium $\eta$-$Cu_6Sn_5$ IMCs layer grow thicker at the Cu/Sn interface, given sufficient Cu supply and relatively longer interaction time.

Accelerated ageing allowed the nano-scale non-equilibrium metastable phases to be fully homogenised towards the equilibrium status as observed by cross-sectional TEM. While the pronounced nano-scale IMCs precipitates exist prior to or after short time (e.g. 5 mins) ageing, with the extended ageing time, the merging and subsequent growth of these original IMCs are apparent. This is driven by the solid-diffusion of Cu and Ag atoms into Sn grains, causing the homogenisation of entire Sn—Cu interconnect at elevated temperature. At the NanoFoil/Sn and Cu/Sn interfaces, the IMCs also evolved with ageing time through the concurrent homogenisation and growth of interfacial IMCs, but it significantly differentiates from the kinetics of equilibrium IMCs, for instance, in the case of Sn joints formed by the conventional reflow process.

It has been reflected that the Cu—Sn joints were consolidated as such the shear strengths increased at initial ageing. However, further extended ageing time can deteriorate the mechanical strength of the Sn—Cu interconnects. The fundamental insight into the formation and homogenisation of Sn—Cu interconnects by self-propagating exothermic reactive bonding in this study will effectively guide the design and manufacture of such joints by considering the materials and processing windows.

## CRediT authorship contribution statement

**Wenbo Zhu:** Conceptualization, Methodology, Software, Validation, Formal analysis, Investigation, Data curation, Writing - original draft, Visualization. **Xiaoting Wang:** Methodology, Software, Formal analysis, Data curation. **Changqing Liu:** Conceptualization, Resources, Writing - review & editing, Visualization, Supervision, Project administration, Funding acquisition. **Zhaoxia Zhou:** Methodology, Resources, Formal analysis, Writing - review & editing. **Fengshun Wu:** Conceptualization, Resources, Writing - review & editing, Supervision, Project administration, Funding acquisition.

## Acknowledgments

The authors acknowledge the studentship jointly awarded by Loughborough University (UK) and Huazhong University of Science and Technology, HUST (China), as well as two research grants on "quasi-ambient bonding (QAB)" (Ref: EP/R032203/1) and "heterogeneous integration (HI)" (Ref: EP/R004501/1) funded by EPSRC of the United Kingdom. The research was also partially supported by a research grant of the National Natural Science Foundation of China (NSFC NO. 61574068) and the Fundamental Research Funds for the Central Universities (No. 2016JCTD112). The State Key Laboratory of Materials Processing and Die & Mold Technology in HUST, as well as the Loughborough Materials Characterization Centre have also supported this work by the provision of the relevant analytical and testing services.

## References

[1] J. Braeuer, J. Besser, M. Wiemer, T. Gessner, A novel technique for MEMS packaging: reactive bonding with integrated material systems, Sensors Actuators A Phys. 188 (2012) 212–219.
[2] T. Matsuda, M. Takahashi, T. Sano, A. Hirose, Multiple self-exothermic reactions for room-temperature aluminum bonding via instantaneous melting, Mater. Des. 121 (Complete) (2017) 136–142.
[3] T. Matsuda, M. Takahashi, T. Ogura, T. Sano, A. Hirose, Self-heating bonding of A5056 aluminum alloys using exothermic heat of combustion synthesis, Mater. Des. 113 (2017) 109–115.
[4] B. Boettge, J. Braeuer, M. Wiemer, M. Petzold, J. Bagdahn, T. Gessner, Fabrication and characterization of reactive nanoscale multilayer systems for low-temperature bonding in microsystem technology, J. Micromech. Microeng. 20 (2010), 064018.
[5] J. Zhang, F.-s. Wu, J. Zou, B. An, and H. Liu, "Al/Ni multilayer used as a local heat source for mounting microelectronic components," in electronic packaging Technology & High Density Packaging, 2009. ICEPT-HDP'09. International Conference on, 2009, 838–842.
[6] J. Wang, E. Besnoin, O.M. Knio, T.P. Weihs, Effects of physical properties of components on reactive nanolayer joining, J. Appl. Phys. 97 (11) (2005) 1262.
[7] T. Jensen., "NanoFoil properties," Indium Corporation, Available: http://www.indium.com/NanoFoil/properties/.
[8] R. Pretorius, A. Vredenberg, F. Saris, R. De Reus, Prediction of phase formation sequence and phase stability in binary metal-aluminum thin-film systems using the effective heat of formation rule, J. Appl. Phys. 70 (1991) 3636–3646.
[9] Y. Wang, Z.-K. Liu, L.-Q. Chen, Thermodynamic properties of Al, Ni, NiAl, and Ni 3 Al from first-principles calculations, Acta Mater. 52 (2004) 2665–2671.
[10] Matthias P. Kremer, A. Roshanghias, A. Tortschanoff, Self-propagating reactive Al/Ni nanocomposites for bonding applications, Micro and Nano Systems Letters 5 (1) (2017) 12.
[11] J. Wang, E. Besnoin, A. Duckham, S.J. Spey, Joining of stainless-steel specimens with nanostructured Al/Ni foils, J. Appl. Phys. 95 (2004) 248–256.
[12] T. Fiedler, I.V. Belova, S. Broxtermann, G.E. Murch, A thermal analysis on self-propagating high temperature synthesis in joining technology, Comput. Mater. Sci. 53 (2012) 251–257.
[13] L. Motiei, Y. Yao, J. Choudhury, H. Yan, T.J. Marks, M.E.v.d. Boom, A. Facchetti, Self-propagating molecular assemblies as interlayers for efficient inverted bulk-heterojunction solar cells, J. Am. Chem. Soc. 132 (2010) 12528–12530.
[14] R. Grieseler, T. Welker, J. Müller, P. Schaaf, Bonding of low temperature cofired ceramics to copper and to ceramic blocks by reactive aluminum/nickel multilayers, Phys. Status Solidi A 209 (2012) 512–518.
[15] C. Pascal, R. Marin-Ayral, J. Tedenac, Joining of nickel monoaluminide to a superalloy substrate by high pressure self-propagating high-temperature synthesis, J. Alloys Compd. 337 (2002) 221–225.
[16] J.S. Kim, T. Lagrange, B.W. Reed, R. Knepper, T.P. Weihs, N.D. Browning, G.H. Campbell, Direct characterization of phase transformations and morphologies in moving reaction zones in Al/Ni nanolaminates using dynamic transmission electron microscopy, Acta Mater. 59 (2011) 3571–3580.

[17] W. Zhu, F. Wu, B. Wang, E. Hou, P. Wang, C. Liu, W. Xia, Microstructural and mechanical integrity of Cu/Cu interconnects formed by self-propagating exothermic reaction methods, Microelectron. Eng. 128 (2014) 24–30.
[18] Heat transfer module. COMSOL, Available: https://www.comsol.com/heat-transfer-module.
[19] Wenbo Zhu, Soldering interconnects through self-propagating reaction process, PhD. Thesis, Loughborough University, UK, 2016.
[20] Florence Baras, Vladyslav Turlo, Olivier Politano, Sergey Georgievich Vadchenko, Alexander Sergeevich Rogachev, Alexander Sergeevich Mukasyan, "SHS in Ni/Al nanofoils: a review of experiments and molecular dynamics simulations", Adv. Eng. Mater., 2018, vol. 20(8), 1800091.
[21] Shengyan Shang, Anil Kunwar, Yanfeng Wang, Jinye Yao, Yingchao Wu, Haitao Ma, Yunpeng Wang, Geometrical effects of Cu@Ag Core-Shell nanoparticles treated flux on the growth behaviour of Intermetallics in Sn/Cu solder joints, Electron. Mater. Lett. 15 (2019) 253–265.
[22] T. Gancarz, Z. Moser, W. G?Sior, J. Pstru?, H. Henein, A comparison of surface tension, viscosity, and density of Sn and Sn–Ag alloys using different measurement techniques, Int. J. Thermophys. 32 (6) (2011) 1210–1233.
[23] W. Kurz, B. Giovanola, R. Trivedi, Theory of microstructural development during rapid solidification, Acta Metall. 34 (1986) 823–830.
[24] R. Nakamura, K. Fujita, Y. Iijima, M. Okada, Diffusion mechanisms in B2 NiAl phase studied by experiments on Kirkendall effect and interdiffusion under high pressures, Acta Mater. 51 (2003) 3861–3870.
[25] Kaustubh N. Kulkarni, Diffusion in B2 NiAl and FeAl intermetallics and their alloys, Diffusion Foundations 13 (2017) 98–135.
[26] B.J.S. de Bas, Simulation of Bulk and Grain Boundary Diffusion in B2 NiAl, Virginia Polytechnic Institute and State University, 2001.
[27] J. Haimovich, Cu-Sn intermetallic compound growth in hot-air-leveled tin at and below 100 C, AMP Journal of Technology 3 (1993) 46–54.
[28] X. Li, T. Ivas, A.B. Spierings, K. Wegener, C. Leinenbach, Phase and microstructure formation in rapidly solidified cu-sn and cu-sn-ti alloys, J. Alloys Compd. 735 (2017) 1374–1382.
[29] S. Ojha, Metastable phase formation during solidification of undercooled melt, Mater. Sci. Eng. A 304 (2001) 114–118.
[30] M. Schweizer, L. Sagis, Nonequilibrium thermodynamics of nucleation, J. Chem. Phys. 141 (2014), 224102.
[31] I. Ovid'ko, A. Sheinerman, E. Aifantis, Stress-driven migration of grain boundaries and fracture processes in nanocrystalline ceramics and metals, Acta Mater. 56 (2008) 2718–2727.
[32] T. Rupert, D. Gianola, Y. Gan, K. Hemker, Experimental observations of stress-driven grain boundary migration, Science 326 (2009) 1686–1690.
[33] T. Takenaka, M. Kajihara, Fast penetration of Sn into Ag by diffusion induced recrystallization, Mater. Trans. 47 (2006) 822–828.
[34] H. Xing, X. Dong, J. Wang, K. Jin, Orientation dependence of columnar dendritic growth with sidebranching behaviors in directional solidification: insights from phase-field simulations, Metall. Mater. Trans. B 49 (4) (2018) 1547–1559.
[35] H. Dong, Y.Z. Chen, G.B. Shan, Z.R. Zhang, On the nonequilibrium interface kinetics of rapid coupled eutectic growth, Metall. Mater. Trans. A 48 (8) (2017) 3823–3830.
[36] S. Wang, C. Liu, Study of interaction between Cu-Sn and Ni-Sn interfacial reactions by Ni-Sn3.5Ag-Cu sandwich structure, J. Electron. Mater. 32 (2003) 1303–1309.
[37] N. Bao, X. Hu, Y. Li, X. Jiang, Effects of thermal aging on growth behavior of interfacial intermetallic compound of dip soldered Sn/Cu joints, J. Mater. Sci. Mater. Electron. 29 (10) (2018) 8863–8875.
[38] W. Kurz, B. Giovanola, R. Trivedi, Theory of microstructural development during rapid solidification, Acta Metall. 34 (1986) 823–830.
[39] V.A. Baheti, P. Kumar, A. Paul, Effect of Au, Pd and Pt addition in Cu on the growth of intermetallic compounds and the Kirkendall voids in the Cu–Sn system, Journal of Materials Science Materials in Electronics 28 (22) (2017) 17014–17019.